Surveillance of nuclear-restricted pre-ribosomes within a subnucleolar region of *Saccharomyces cerevisiae*

Christophe Dez, Jonathan Houseley and David Tollervey*

Wellcome Trust Centre for Cell Biology, University of Edinburgh, Edinburgh, UK

We previously hypothesized that HEAT-repeat (<u>H</u>untington, <u>e</u>longation <u>A</u> subunit, <u>T</u>OR) ribosome synthesis factors function in ribosome export. We report that the HEAT-repeat protein Sda1p is a component of late 60S pre-ribosomes and is required for nuclear export of both ribosomal subunits. In strains carrying the ts-lethal *sda1–2* mutation, pre-60S particles were rapidly degraded following transfer to 37°C. Polyadenylated forms of the 27S pre-rRNA and the 25S rRNA were detected, suggesting the involvement of the <u>T</u>rf4p/<u>A</u>ir/<u>M</u>tr4p polyadenylation complex (TRAMP). The absence of Trf4p suppressed polyadenylation and stabilized the pre-rRNA and rRNA. The absence of the nuclear exosome component Rrp6p also conferred RNA stabilization, with some hyperadenylation. We conclude that the nuclear-restricted pre-ribosomes are polyadenylated by TRAMP and degraded by the exosome. In *sda1–2* strains at 37°C, pre-40S and pre-60S ribosomes initially accumulated in the nucleoplasm, but then strongly concentrated in a subnucleolar focus, together with exosome and TRAMP components. Localization of pre-ribosomes to this focus was lost in *sda1–2* strains lacking Trf4p or Rrp6p. We designate this nucleolar focus the No-body and propose that it represents a site of pre-ribosome surveillance.

Introduction

Ribosome synthesis largely occurs within the nucleolus but late maturation steps take place in the nucleoplasm, following release of the pre-ribosomes from the nucleolus, and in the cytoplasm, following nucleocytoplasmic export; reviewed in Venema and Tollervey (1999), de la Cruz *et al* (2003), Fromont-Racine *et al* (2003) and Dez and Tollervey (2004).

*Corresponding author. Institute of Cell and Molecular Biology, University of Edinburgh, University of Edinburgh, Swann Building, King's Buildings, Mayfield Road, Edinburgh EH9 3JR, UK.
Tel.: +44 131 650 7092; Fax: +44 131 650 7040;
E-mail: d.tollervey@ed.ac.uk

During maturation, a complex processing pathway converts the 35S pre-rRNA into the mature 18S, 5.8S and 25S rRNAs (see Figure 1A and Supplementary Figure S1), whereas the 5S rRNA is independently transcribed.

The pre-ribosomal subunits are exported through the nuclear pore complex (NPC) to the cytoplasm prior to final maturation. In fast-growing strains of yeast, each NPC exports around 25–30 ribosomal subunits per minute, implying a very efficient transport mechanism. Ribosomal subunit export requires several pre-ribosomal proteins, as well as the exportin Crm1p/Xpo1p (Ho *et al*, 2000; Gadal *et al*, 2001; Moy and Silver, 2002; Thomas and Kutay, 2003; Trotta *et al*, 2003; Oeffinger *et al*, 2004), suggesting that multiple factors are required to allow effective transport of the ribosomal subunits.

Free diffusion of molecules through the lumen of the NPC is restricted by the hydrophobic, FG-repeat regions of nucleoporins (Ribbeck and Gorlich, 2002; Gorlich *et al*, 2003). The translocation of large molecules through the NPC is strongly inhibited unless they can interact with the FG-repeats. However, ribosome subunits are large, highly structured and have many exposed, hydrophilic rRNA regions, and are very unlikely to interact favorably with the NPC. The ability to pass through the lumen of the NPC can be conferred by association with members of the importin-β/karyopherin-β family of transport factors, which consist of repeated, predominantly α-helical motifs termed HEAT-repeats (<u>H</u>untington, <u>e</u>longation <u>A</u> subunit, <u>T</u>OR) that are related to Armadillo-like repeats (Andrade *et al*, 2001). We previously identified a family of ribosome synthesis factors that are made up of HEAT-repeats, and predicted that they would function in ribosomal subunit export (Dlakic and Tollervey, 2004; Oeffinger *et al*, 2004). Specifically we suggested that these factors might form extended structures that help cover the hydrophilic RNA surfaces of the ribosomal subunits, allowing their passage through the hydrophobic mesh formed by the FG-repeats (Dlakic and Tollervey, 2004; Oeffinger *et al*, 2004). Consistent with this model, four of the HEAT-repeat ribosome synthesis factors (Noc2p, Noc3p, Noc4p and Rrp12p) were shown to be required for subunit export, while Noc1p was implicated in intranuclear movement of the pre-ribosomes (Milkereit *et al*, 2001, 2003; Oeffinger *et al*, 2004). Moreover, Rrp12p was shown to interact directly with FG-repeat nucleoporins, Ran and RNA (Oeffinger *et al*, 2004).

Yeast strains with defects in ribosome synthesis generally fail to accumulate high levels of the pre-rRNAs, indicating that an active surveillance system exists but little is known about the mechanisms involved; reviewed in Venema and Tollervey (1999). A key player in RNA degradation is the exosome complex of 3′–5′ exonucleases (Mitchell *et al*, 1997). In the nucleus, the exosome is implicated in elimination of defective pre-mRNAs (Bousquet-Antonelli *et al*, 2000;
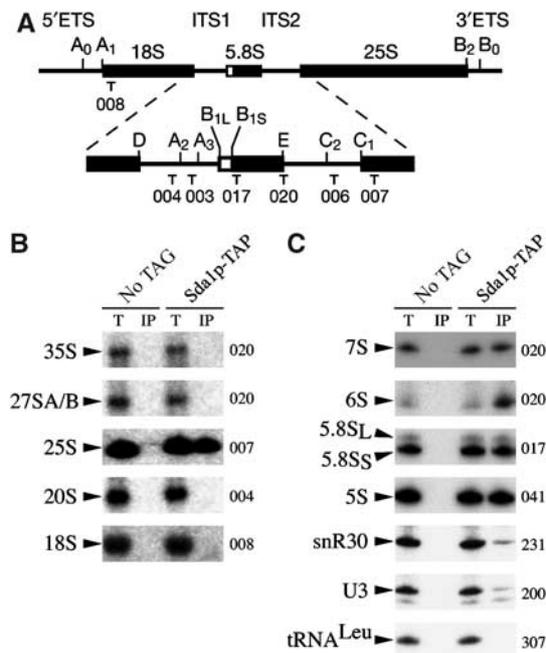
Figure 1 Sda1p is a component of late nuclear 60S pre-ribosomes. (**A**) The 35S pre-rRNA contains the sequences of the mature 18S, 5.8S and 25S rRNAs, which are separated by internal transcribed spacers 1 and 2 (ITS1 and ITS2) and flanked by the 5′ and 3′ external transcribed spacers (5′ETS and 3′ETS). Location of the different oligonucleotides used in this study is shown. (**B, C**) Northern analysis of rRNAs co-precipitated with Sda1-TAP or from extracts of cells lacking a tagged protein. Immunoprecipitation was performed on cell extracts using IgG-Sepharose. RNAs were extracted from the pellet after precipitation (lanes IP) or from an amount of cell extract corresponding to 1/20 (B, 1.2% denaturing agarose gel) or 1/10 (C, 8% polyacrylamide/urea gel) of the total amount used for the precipitations (lanes T). Following separation, RNAs were transferred to a nylon membrane and hybridized with the antisense oligonucleotides indicated to the right of each panel.

Hilleren *et al*, 2001; Torchet *et al*, 2002; Zenklusen *et al*, 2002; Milligan *et al*, 2005; Wyers *et al*, 2005), pre-tRNAs (Kadaba *et al*, 2004; Vanacova *et al*, 2005) and pre-rRNAs (Zanchin and Goldfarb, 1999; Allmang *et al*, 2000; Libri *et al*, 2002; Fang *et al*, 2004; LaCava *et al*, 2005). The activity of the nuclear exosome is stimulated by the TRAMP4 and TRAMP5 complexes (Trf/Air/Mtr4 polyadenylation complex) (Haracska *et al*, 2005; LaCava *et al*, 2005; Vanacova *et al*, 2005; Wyers *et al*, 2005; Houseley and Tollervey, 2006), which include a nuclear poly(A) polymerase, either Trf4p or Trf5p, respectively (Saitoh *et al*, 2002), the putative RNA helicase Mtr4p (Liang *et al*, 1996; de la Cruz *et al*, 1998) and one of two redundant zinc-knuckle proteins Air1p and Air2p (Inoue *et al*, 2000). Consistent with a widespread role for the TRAMP complexes in RNA surveillance, the polyadenylation of precursors to snoRNAs, snRNAs, tRNA and rRNA has been reported (Allmang *et al*, 1999; van Hoof *et al*, 2000; Fang *et al*, 2004; Kadaba *et al*, 2004; Kuai *et al*, 2004; Wyers *et al*, 2005).

We report here the characterization of a surveillance and degradation pathway for ribosome subunits that fail to be exported due to a defect in the HEAT-repeat pre-ribosome component Sda1p. This process appears to occur preferentially within a subnucleolar structure, the No-body, and is mediated by the exosome following TRAMP-dependant polyadenylation of the rRNA substrates.

Results

Sda1p is a component of late 60S pre-ribosomes

Previous proteomic analyses identified Sda1p as a putative component of 60S pre-ribosomes (Baßler *et al*, 2001; Gavin *et al*, 2002). To confirm this interaction, we analyzed RNA species that co-precipitated with epitope-tagged Sda1p, expressed under the control of its own promoter (Sda1-TAP; see Supplementary Table S1) (Rigaut *et al*, 1999). Following immunoprecipitation (see Materials and methods), bound RNAs were analyzed by Northern hybridization and compared with RNAs recovered in parallel from the nontagged control strain (Figure 1B and C). The 7S and 6S pre-rRNAs and the 25S, 5.8S and 5S rRNAs were efficiently co-precipitated with Sda1-TAP. These results are consistent with reports that Sda1p localizes to the nucleolus and nucleoplasm (Buscemi *et al*, 2000; Babbio *et al*, 2004), since 7S pre-rRNA is predominantly nucleolar, whereas the final maturation of 25S and 5.8S rRNA occurs in the nucleoplasm. This suggests that Sda1p associates with 60S pre-ribosomes during late nucleolar maturation steps and accompanies them into the nucleoplasm. Phosphorimager quantification indicated that approximately 5% of the total 25S rRNA population was bound with Sda1-TAP in the experiment shown in Figure 1B. This value would be consistent with previous reports that pre-60S particles undergo relatively slow conversion into mature 60S ribosomes after 25S rRNA synthesis (Tollervey *et al*, 1993). Together, these observations strongly indicate a role for Sda1p in late nuclear steps of 60S ribosome biogenesis.

sda1–2 temperature-sensitive (ts) mutants exhibit a very fast ribosome export defect phenotype

To assess the requirement for Sda1p in subunit export, we used the *sda1–2* ts mutation (Zimmerman and Kellogg, 2001). The mutant and isogenic wild-type strains were transformed with CEN plasmids expressing GFP-tagged ribosomal proteins Rps2-GFP (40S subunit component), Rpl11b-GFP or Rpl25-GFP (60S subunit components) (Stage-Zimmermann *et al*, 2000; Grandi *et al*, 2002). Under permissive conditions (23°C), Rps2-GFP (Figure 2A), Rpl11b-GFP (Figure 2B) and Rpl25-GFP (data not shown) were predominantly found throughout the cell in both wild-type and *sda1–2* strains. The *sda1–2* cells growing at 23°C showed a mild growth defect (t_2 2.9 h for *sda1–2* versus 1.7 h for wt) and around 5% showed detectable nuclear enrichment of Rps2-GFP, Rpl11b-GFP and Rpl25-GFP (data not shown). Cultures were shifted to 37°C by transfer to prewarmed flasks in a water bath. Following transfer, a very rapid inhibition of subunit export was observed. After 5 min at 37°C, over 80% of *sda1–2* cells showed a strong nucleoplasmic accumulation of Rps2-GFP, Rpl11b-GFP and Rpl25-GFP (Figure 2A and B and data not shown). Sda1–2p is stable for at least 5 h at the nonpermissive temperature (Zimmerman and Kellogg, 2001), indicating that the protein is present but impaired in function. We conclude that functional Sda1p is required for efficient export of both pre-40S and pre-60S ribosomal subunits from the nucleoplasm to the cytoplasm.

A

Rps2-GFP   DAPI   Merge

SDA1

23°C

5 min at 23°C

sda1-2

23°C

5 min at 23°C

B

Rpl11b-GFP   DAPI   Merge

SDA1

23°C

5 min at 23°C

sda1-2

23°C

5 min at 23°C
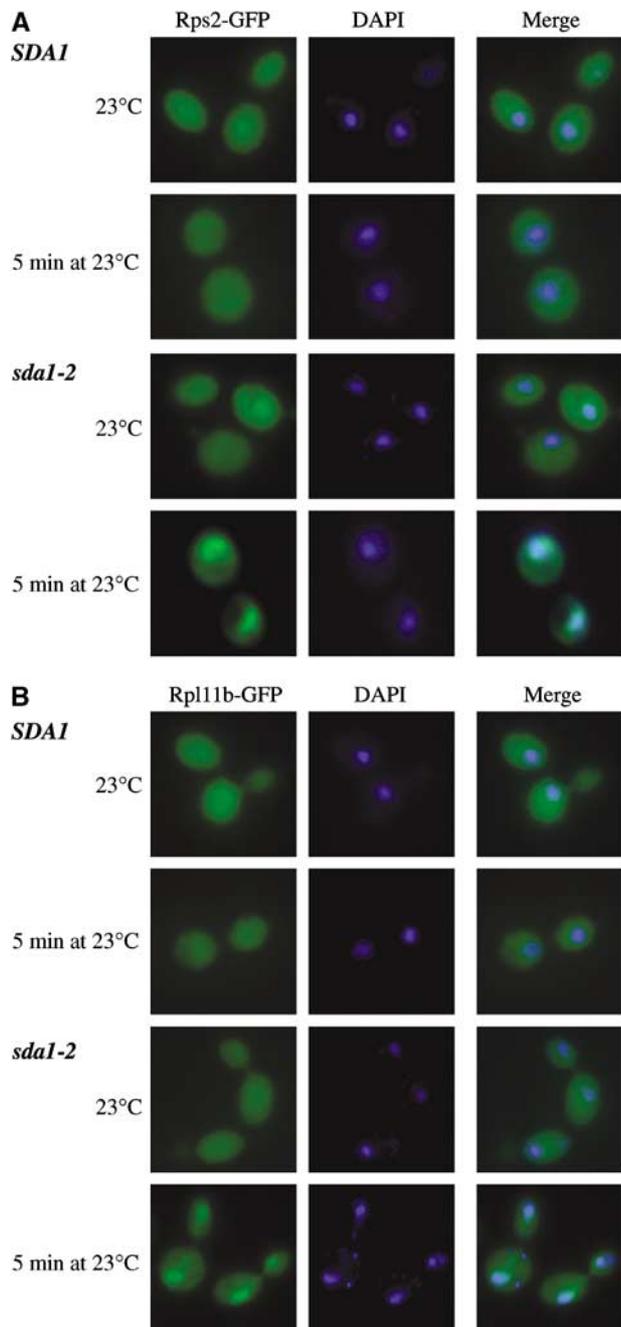
Figure 2 The *sda1–2* mutant shows a rapid block in 40S and 60S subunit export. Analysis of 40S and 60S subunit export in *sda1–2* strains expressing Rps2-GFP (**A**) or Rpl11b-GFP (**B**) reporter construct. Cells were pregrown at 23°C and then shifted to 37°C for 5 min. Cells were fixed, DAPI stained and viewed by fluorescence microscopy.

Sda1p is required for 60S ribosomal subunit maturation and accumulation

The fast and complete inhibition of export in *sda1–2* strains allows us to relate the behavior of individual cells visualized in microscopy to RNA metabolism in the entire population, which was assessed by Northern hybridization (Figure 3A and B) and metabolic labeling (Figure 4).

RNA was harvested from cells growing at 23°C, and at time points after transfer to 37°C. Northern hybridization (Figure 3A and B, lanes 1–10) revealed strong pre-rRNA accumulation defects in the *sda1–2* strain 15–30 min after transfer to

the restrictive temperature. Defects were most evident in the pathway leading to 25S rRNA synthesis, with substantial reductions in the levels of 35S and 27S pre-rRNAs as well as 25S mature rRNA (Figure 3A). Since an equal amount of total RNA was loaded in each lane, reduced levels of the very abundant rRNAs leads to overloading of the lanes when equal amounts of total RNA are loaded. Pre-rRNAs and rRNAs were therefore quantified relative to the scR1 RNA, the RNA component of the cytoplasmic signal recognition particle (SRP). The 35S and 27S pre-rRNA levels were reduced by 60% after 30 min at 37°C and by 80% after 1 h, while mature 25S rRNA was reduced by 25 and 45% (Figure 3C). Analysis of the same RNA preparations showed accumulation of the 7S pre-rRNA (five-fold after 30 min), accompanied by 1.5-fold underaccumulation of the mature 5.8S rRNAs (Figure 3B). The reduction in 25S levels was clearly more rapid than that of 5.8S rRNA. A similar observation was made for strains depleted of another HEAT-repeat protein Rrp12p (Oeffinger *et al*, 2004), suggesting that 25S rRNA is more rapidly degraded than 5.8S rRNA when export is inhibited.

Relative to the scR1 RNA loading control, the 20S pre-rRNA accumulated 2.5-fold in *sda1–2* ts mutants after 1 h at 37°C, whereas accumulation of the 18S rRNA was reduced by 25% (Figure 3A and C). The conversion of 20S pre-rRNA into mature 18S rRNA occurs in the cytoplasm, suggesting that this phenotype is a consequence of the 40S subunit export defect observed *sda1–2* strains (Figure 2A). The signals for all snoRNAs tested were also increased in the *sda1–2* strain (Figure 3B), presumably reflecting reduced levels of the rRNAs.

Pre-rRNA processing in *sda1–2* strains was also analyzed by pulse-chase labeling with [³H]adenine, commencing 5 min after temperature shift (Figure 4, lanes 1–12). Probably as a consequence of a rapid shift to 37°C, global pre-rRNA processing in both wild-type and *sda1–2* strains was slower than is usually observed. Total incorporation of label was lower in each of the *sda1–2* strains than the wild type (in Figure 4 the wild-type lanes are exposed four-fold less than the other panels), presumably due to the reduced growth rate prior to the temperature shift. Consistent with the Northern data, production of mature 18S rRNA was delayed in *sda1–2* strain at 37°C relative to the wild-type strain (compare lanes 5 and 11), whereas 25S rRNA synthesis was strongly impaired. Notably, despite the substantial reduction in 25S accumulation, the appearance and loss of 27S pre-rRNA was relatively similar in both strains. This observation indicates that 27S pre-rRNA was synthesized in *sda1–2* strains at 37°C, but the 27S pre-rRNA and/or the mature 25S were then degraded. The 7S pre-rRNA accumulation seen by Northern blot (Figure 3, lanes 6–10) and pulse-chase labeling (Figure 4B) shows that at least some of the 27SB pre-rRNA population continues to undergo endonuclease cleavage at site C$_2$.

We conclude that newly synthesized 25S rRNA and probably part of 27SB pre-rRNA population were degraded in the *sda1–2* mutant at 37°C. Maturation of 20S pre-rRNA to 18S rRNA was slowed and 18S rRNA accumulation was reduced, consistent with slowed export.

The loss of TRAMP or exosome activities stabilizes 27S pre-rRNA and 25S rRNA

We speculated that the TRAMP and exosome complexes degrade the 27SB pre-rRNA and/or 25S rRNA in *sda1–2*
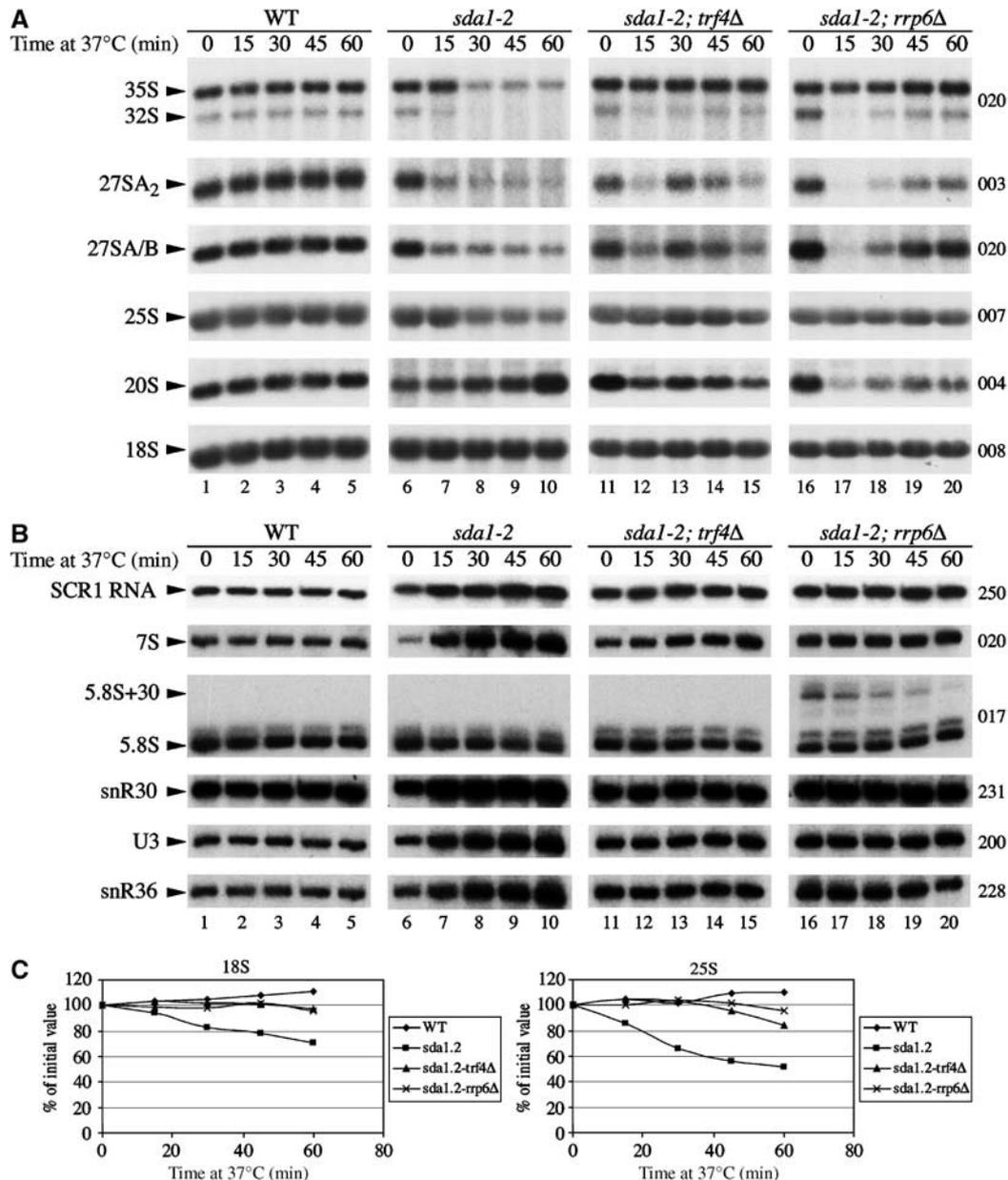
Figure 3 Northern analyses of pre-rRNA processing in *sda1–2* mutant strains. Levels of pre-rRNAs and rRNAs were assessed by Northern blotting. Cells were pregrown at 23°C and transferred to 37°C. Samples were collected at 23°C (lanes 1, 6, 11 and 16) and after transfer to 37°C for 15 min (lanes 2, 7, 12 and 17), 30 min (lanes 3, 8, 13 and 18), 45 min (lanes 4, 9, 14 and 19) and 60 min (lanes 5, 10, 15 and 20). RNA was extracted and separated on denaturing 1.2% agarose gels (**A**) or on 8% polyacrylamide/urea gels (**B**) and transferred to a nylon membrane. Oligonucleotides used for Northern hybridization are indicated to the right of each panel (see Figure 1A for locations of oligos). (**C**) Quantification of data in panel A, standardized to the level of scR1 RNA.

strains. We therefore created *sda1–2* strains that also carry *rrp6Δ*, which eliminates a nuclear-specific exosome component, or *trf4Δ*, which eliminates the poly(A) polymerase component of the TRAMP4 complex. Northern analyses (Figure 3) showed that the absence of either Rrp6p or Trf4p partially rescued the (pre-)rRNA accumulation defect observed in *sda1–2* single mutants. Accumulation of the 25S rRNA in *sda1–2, trf4Δ* and *sda1–2, rrp6Δ* strains was close to wild-type levels after the temperature shift (Figure 3). The 27S pre-rRNA pattern was more difficult to interpret, particularly in the *sda1–2, rrp6Δ* strain, which showed a precipitous decline in pre-rRNA levels 15 min after transfer to 37°C. The basis of this is not clear, but we have also seen dramatic,

transient reductions in mRNA levels immediately following transfer of exosome mutants to 37°C (Milligan *et al*, 2005). However, 1 h after transfer to 37°C, 27S pre-rRNA levels were reduced by only 10% in *sda1–2, rrp6Δ* and by 31% in *sda1–2, trf4Δ*, compared to a 80% reduction in the *sda1–2* single mutant. The reduced 35S RNA levels seen in the *sda1–2* strain was also largely suppressed in the strains also lacking Rrp6p or Trf4p. Sda1p is not predicted to be associated with 35S pre-rRNA, and we speculate that its reduction may be an indirect effect of activation of a pre-rRNA surveillance pathway, which is suppressed in the double mutants.

Pulse-chase analyses of the *sda1–2, trf4Δ* and *sda1–2, rrp6Δ* strains revealed stabilization of the 27S pre-rRNA and
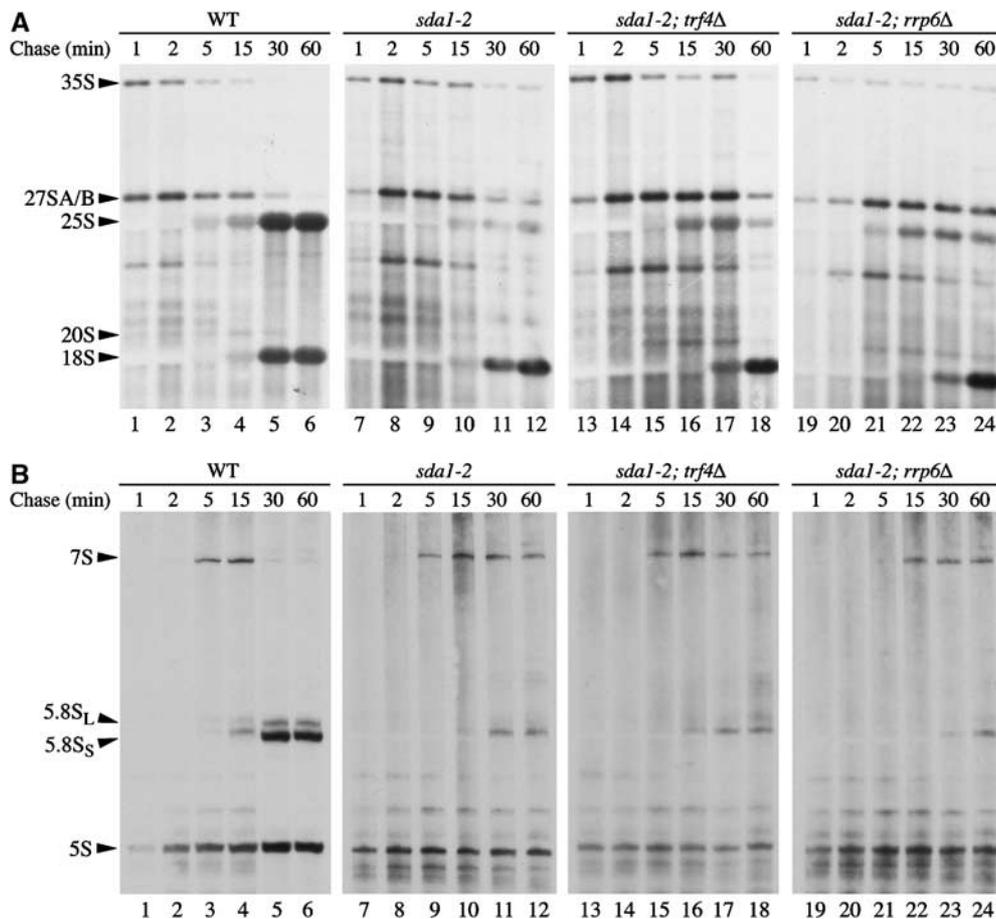
Figure 4 Pulse-chase analyses of pre-rRNA processing in *sda1–2* mutant strains. Cultures were pregrown at 23°C and transferred to 37°C for 5 min. Cells were then pulse labeled with [³H]adenine for 2 min, followed by the addition of an excess of cold adenine. Samples were collected at the times indicated, and RNAs were extracted, separated on a denaturing 1.2% agarose gel (**A**) or a 8% polyacrylamide/urea gel (**B**) and transferred to a nylon membrane. Labeled RNAs were detected by fluorography. The exposure shown for the wild-type samples is four-fold shorter than the other panels.

25S rRNA relative to the *sda1–2* single mutant (Figure 4). In the *sda1–2* single mutant, the 27S pre-rRNA signal dropped 15 min after the chase, whereas in the absence of Trf4p or Rrp6p it appeared much more stable. Accumulation of the mature 25S rRNA was also higher in the double mutants compared to *sda1–2* single mutant. However, the *trf4Δ* and *rrp6Δ* mutations did not allow growth of *sda1–2* strains at 37°C (data not shown), possibly because the 60S ribosomes remain trapped in the nucleus (see below). Consistent with the Northern data, the 7S pre-rRNA was much more stable than the 27S pre-rRNAs in the *sda1–2* strains, and was not clearly further stabilized by the *rrp6Δ* or *trf4Δ* mutations. Also consistent with the Northern data, accumulation of the 18S rRNA was similar in *sda1–2* strains with or without Rrp6p or Trf4p, indicating that it does not undergo substantial degradation by TRAMP/exosome activity.

These results indicate that the degradation of the 27S pre-rRNA and 25S rRNA observed in *sda1–2* strains requires the TRAMP complex and the nuclear exosome.

The 27S pre-rRNA and 25S rRNA undergo TRAMP-dependent polyadenylation in sda1–2 strains

The apparent involvement of the TRAMP complex in pre-ribosome degradation suggested the RNAs might undergo polyadenylation by the poly(A) polymerase activity of Trf4p

prior to degradation by the exosome. To test this hypothesis, we analyzed the accumulation of polyadenylated RNA in *sda1–2* mutant strains. RNA was extracted from strains growing at 23°C and at time points following transfer to 37°C, fractionated by oligo(dT) selection and analyzed by Northern hybridization (Figure 5). In the wild type (Figure 5, lanes 1–5), a low level of polyadenylated pre-rRNA was detected, as previously reported (Fang *et al*, 2004; Kuai *et al*, 2004). This did not comigrate with either the 27S pre-rRNA or 25S rRNA, and presumably reflects a low level of pre-rRNA degradation that normally occurs in wild-type cells. In the *sda1–2* strain (Figure 5, lanes 6–10), polyadenylated forms of 27S and 25S RNA increased following transfer to 37°C, and were estimated to represented around 3% of the total pools. In contrast, the 7S pre-rRNA was not clearly polyadenylated in the *sda1–2* strain (data not shown), consistent with its relative stability following pulse-labeling (Figure 4). The 20S pre-rRNA and 18S rRNA showed no increase in polyadenylated forms that were long enough to be retained on the column (∼A₁₅) following temperature shift. This is consistent with the conclusion that the large ribosomal subunit precursors are preferentially degraded in *sda1–2* strains.

In the strains lacking Trf4p, very little polyadenylated pre-rRNA or rRNA was detected (Figure 5, lanes 21–30).

Overexposure of the Northern blots showed that a small amount of pre-rRNA and rRNA was still retained on the oligo(dT) column in the *trf4Δ* strains but the levels appeared to be independent of *sda1–2* and temperature variation (data

not shown). We concluded that polyadenylation of pre-rRNAs and rRNAs in *sda1–2* mutant is largely the consequence of Trf4p activity. In the strain lacking only Rrp6p (Figure 5, lanes 41–45), polyadenylated forms were detected for all tested pre-rRNAs and rRNAs. Some hyperadenylation of the 27S pre-rRNA was apparent in the *sda1–2, rrp6Δ* strain (Figure 5, lanes 46–50) relative to the *sda1–2* single mutant (Figure 5, lanes 6–10).

From these results we concluded that exosome-mediated degradation of 27S pre-rRNA and 25S rRNA in *sda1–2* mutants involves their prior polyadenylation by the TRAMP4 complex.

Nuclear-restricted pre-ribosomes, TRAMP and the exosome concentrate in a nucleolar focus

As shown above (Figure 2), nuclear accumulation of pre-ribosomes was seen 5 min after transfer to the nonpermissive temperature. However, the Northern analyses indicate that most degradation of the pre-ribosomes occurs after 15–30 min at 37°C. With the aim of determining the site of pre-ribosome degradation, the Rps2-GFP, Rpl11b-GFP and Rpl25-GFP reporters were analyzed in *SDA1* and *sda1–2* strains during 1 h following temperature shift. In wild-type strains, all three r-proteins showed a uniform distribution throughout the nucleus and the cytoplasm (Figures 2 and 6A, and Supplementary Figures S2D and S3A). In *sda1–2* mutant strains, Rps2-GFP, Rpl11b-GFP and Rpl25-GFP each showed a striking pattern of localization. After 5 min at 37°C, the r-proteins accumulated in the nucleoplasm, with no clear nucleolar enrichment (Figures 2 and 6A and data not shown), consistent with a block in transport across the NPC. However, by 15 min after temperature shift, the r-proteins had become strongly enriched in a sharp focus (Figure 6A, Supplementary Figures S2D and S3A). Colocalization with the nucleolar marker Nop1p (Figure 6B) showed this focus to lie within the nucleolus. The focus persisted in the 30 min time point and was present in more than 80% of cells. The same localization was observed in living cells (data not shown). By 60 min after transfer to 37°C, the cell morphology had changed, with the formation of a very large cytoplasmic vacuole, while the nuclear GFP signal appeared weaker and more diffuse. This dynamic localization pattern was similar for both the 40S (Rps2p) and 60S (Rpl11bp and Rpl25p) ribosomal proteins (Figure 6A, Supplementary Figures S2D and S3A and data not shown) and was very reproducible.

The cytoplasmic Rpl11b-GFP signal appeared unaltered in the *sda1–2* strain at early time points after transfer to 37°C, but to fully confirm this, we mixed an equal quantity of *SDA1* and *sda1–2* cells (Supplementary Figure S2C: note that the
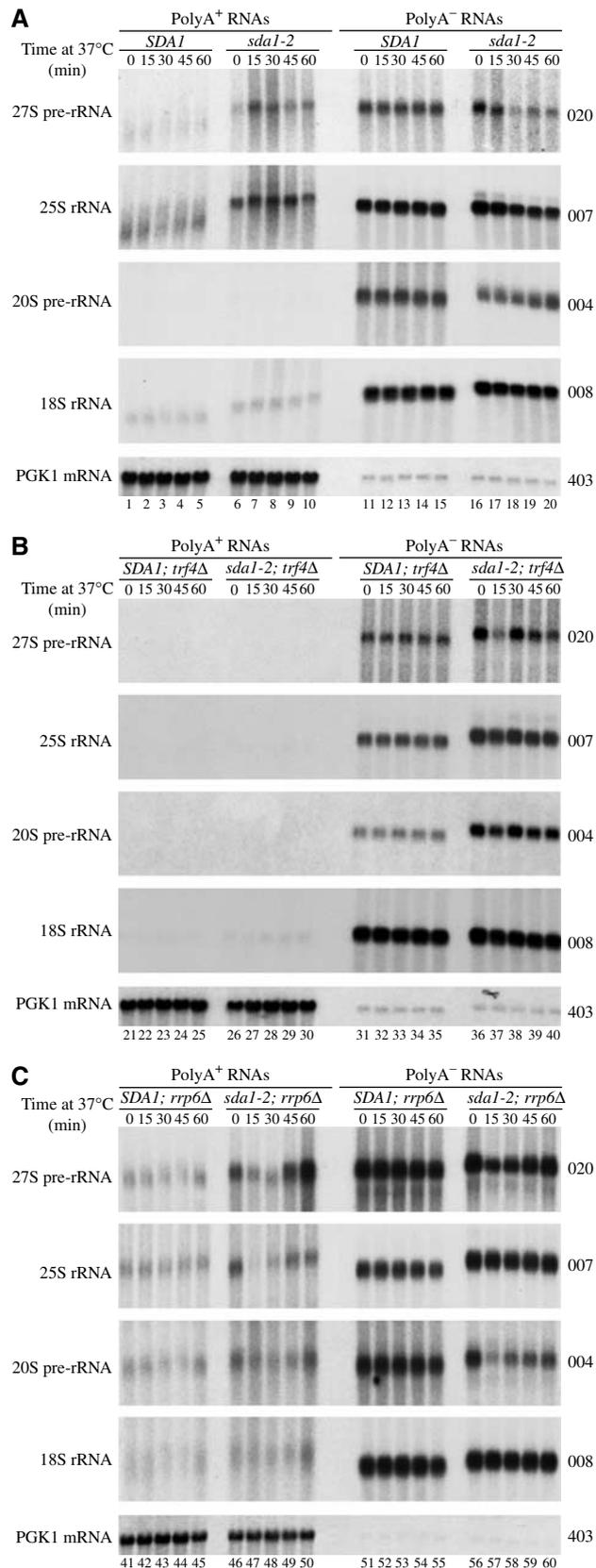
Figure 5 Polyadenylated rRNAs are accumulated in *sda1–2* and *rrp6Δ* mutants but not in strains lacking Trf4p. The same RNA samples as used for Figure 4 were submitted to oligo(dT) selection. The resulting bound (poly(A)$^+$ enriched) and unbound (poly(A)$^+$ depleted) fractions were loaded on a denaturing 1.2% agarose gel and transferred to a nylon membrane. (**A**) Comparison of *SDA1* and *sda1–2* single mutants. (**B**) Comparison of *SDA1* and *sda1–2* in a *trf4Δ* background. (**C**) Comparison of *SDA1* and *sda1–2* in a *rrp6Δ* background. Oligonucleotides used for Northern hybridizations are indicated to the right of each panel. The *PGK1* mRNA was used as a control for loading and polyadenylated RNA selection.
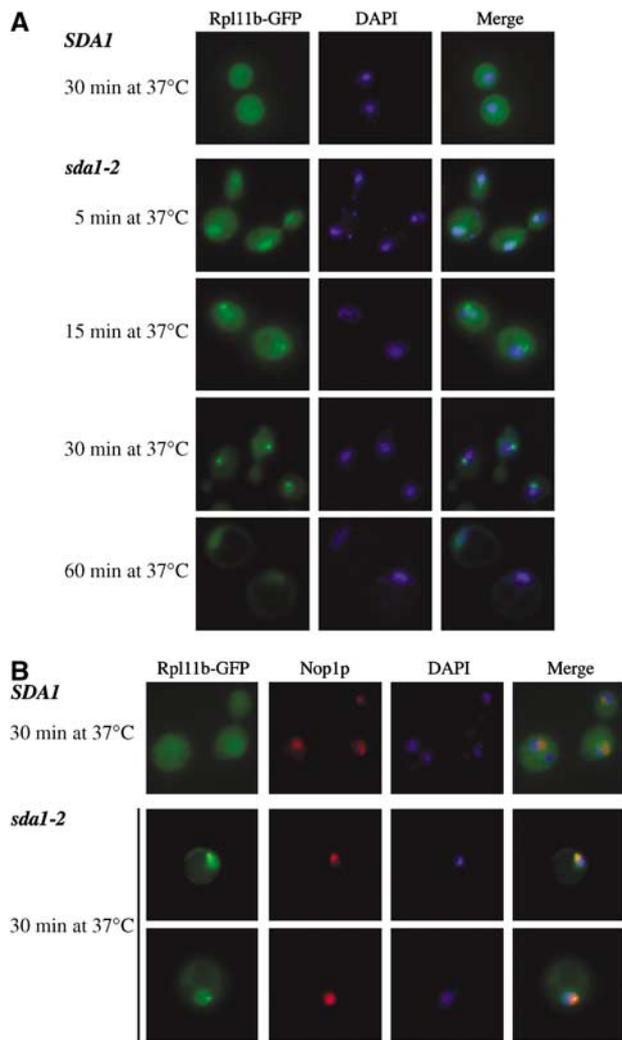
Figure 6 Rpl11p-GFP concentrates in a subnucleolar structure in *sda1–2* strains 15 min after temperature shift. (**A**) Localization of Rpl11b-GFP in *SDA1* wild-type and *sda1–2* ts mutants. Aliquots were collected at different times following temperature shift and cells were fixed before they were viewed in the fluorescence microscope. (**B**) The Rpl11-GFP focus was visualized within the nucleolus using optical microscopy. The nucleolus was visualized using an anti-Nop1p antibody, which was subsequently recognized by an Alexafluor 555-conjugated secondary antibody.

site of pre-ribosome accumulation is out of the focal plane in some of the *sda1–2* cells in the image). Western blotting (Supplementary Figure S2A) showed no substantial alterations in the level of the Rpl11b protein in the *sda1–2* strain following transfer to 37°C.

We next wanted to confirm that the GFP-tagged r-protein reporters were faithfully reporting the site of pre-ribosome accumulation. Sucrose density gradient fractionation showed that nearly all Rps2-GFP and Rpl11b-GFP are associated with pre-ribosomes and ribosomes in *sda1.2* strain following transfer to 37°C (Figure 7A and Supplementary Figure S3B), confirming that the focus does not reflect an accumulation of free r-proteins.

Localization of the pre-rRNA was directly visualized by fluorescent *in situ* hybridization (FISH) as previously described (Bertrand *et al*, 1998) using a Cy3-labeled probe specific for the pre-rRNA ITS2 region (Leger-Silvestre *et al*,
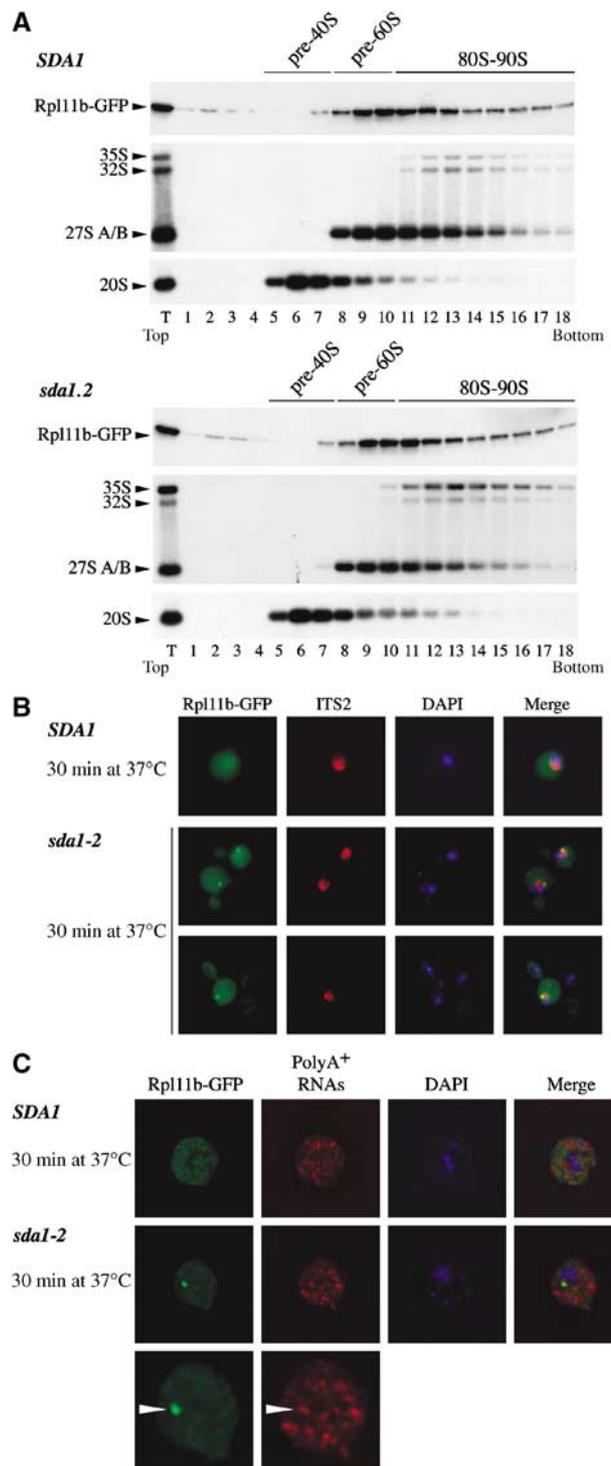
Figure 7 Pre-ribosome components and polyadenylated RNAs concentrate in the subnucleolar substructure. (**A**) Glycerol density gradient analysis of Rpl11p-GFP. A total cellular extract was prepared from wild-type and *sda1.2* strains expressing Rpl11p-GFP, collected 15 min following temperature shift. Samples were loaded on a 10–30% glycerol gradient and 18 fractions were collected. Proteins and RNAs were extracted from the fractions and subjected to Western blot and Northern blot analysis, respectively. T: sample from the total unfractionated extract. (**B**) FISH localization of pre-rRNAs using a Cy3-labeled ITS2 probe (Leger-Silvestre *et al*, 2004). (**C**) FISH localization of polyadenylated RNAs using a Cy5-labeled oligo(dT). Wild-type and *sda1.2* cells expressing Rpl11p-GFP were collected 15 min after temperature shift. Polyadenylated RNAs were imaged using a Deltavision system. These images were subjected to decovolution, and a single optical section is presented in each panel.

2004). This region is present in the early 35S to the 32S pre-rRNAs and is retained in the 27S and 7S pre-rRNAs (see Supplementary Figure S1). In the wild-type cells, the signal was concentrated in the nucleolus and is also detected in the nucleoplasm (Figure 7B). In *sda1–2* strains, clear accumulation of the ITS2 signal was seen in the nucleolar focus, together with weaker nucleolar and nucleoplasmic signals.

Northern data indicated that the 27S pre-rRNA and 25S rRNA undergo polyadenylation in the *sda1–2* strain (Figure 5). We therefore assessed whether the foci were enriched for polyadenylated RNA by FISH analysis, using a Cy5-labeled oligo(dT) probe (Figure 7C). As expected, a strong poly(A) signal was detected throughout the cytoplasm, but a focus was also seen to colocalize with the Rpl11b-signal (images in Figure 7C each show a single optical section through the cells). No clear nuclear poly(A) signal was observed in the wild-type (Figure 7C) or in the *sda1–2* strain at 23°C (data not shown). This observation is consistent with the accumulation of polyadenylated pre-RNA and/or rRNA in the nucleolar focus in *sda1.2* cells.

To assess the colocalization of the degradation machinery with the GFP-tagged r-protein reporters, C-terminal RFP-fusions were constructed for exosome (Rrp45p), TRAMP (Trf4p, Air2p and Mtr4p) or proteasome (Rpn10p and Pre5p) components. These were expressed from the endogenous promoters at the endogenous loci. Strains were harvested and analyzed during growth at 23°C and 15 min after transfer to 37°C (Figure 8). The core exosome component Rrp45-RFP and all three TRAMP components Trf4-RFP, Mtr4-RFP and Air2-RFP each showed a broad distribution throughout the nucleus but were enriched in the pre-ribosome focus in *sda1–2* cells (shown by the yellow spot in the merged panels in Figure 8). We were unable to construct the Rrp6-RFP allele, however, an Rrp6-CFP construct was also enriched in a sharp focus in *sda1–2* mutants (data not shown).

It seemed possible that the r-protein components of the pre-ribosomes might be degraded at the same time as the pre-rRNAs, since this might avoid potentially severe problems associated with the generation of free r-proteins. However, the proteasome components Rpn10-RFP (Figure 8E) and Pre5-RFP (data not shown) were detected throughout the nucleoplasm and nucleolus but showed no enrichment within the focus.

We conclude that the TRAMP and exosome complexes concentrate with the pre-ribosomes within a discrete sub-nucleolar structure, which is also enriched for poly(A) RNA, whereas the proteasome is not enriched in this region.

TRAMP and exosome components are required for the enrichment of pre-ribosomes in a focus

The loss of components of the TRAMP or exosome complexes reduced degradation of the pre-rRNAs and rRNA, and we speculated that this might correlate with reduced concentration of pre-ribosomes in the nucleolar focus. We tested this hypothesis by examining the localization of Rpl11b-GFP in wild-type and *sda1–2* strains lacking either Rrp6p or Trf4p (Figure 9). In *SDA1* cells, the absence of Rrp6p or Trf4p induced no clear change in the localization of Rpl11p, and the GFP signal was distributed throughout the cells (Figure 9). In contrast, the *sda1–2, rrp6Δ* and *sda1–2, trf4Δ* double mutants were distinctly different from the *sda1–2* single mutant.
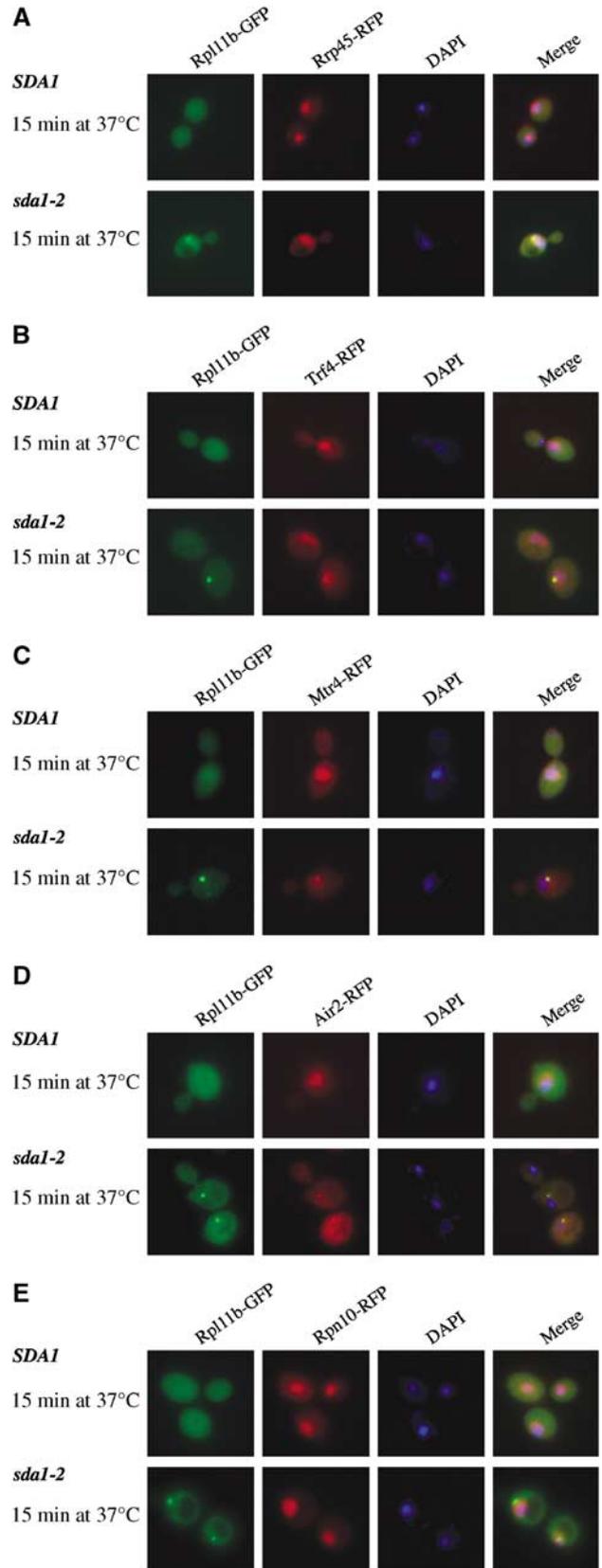
Figure 8 TRAMP and exosome components also concentrate in the same sharp focus in *sda1–2* mutants. RFP-tagged versions of exosome (Rrp45p (**A**)), TRAMP (Trf4p (**B**), Mtr4p (**C**) and Air2p (**D**)) and proteasome (Rpn10p (**E**)) components were expressed in *SDA1* and *sda1–2* strains also expressing Rpl11-GFP. The resulting strains were pregrown at 23°C and shifted to 37°C for 15 min. Cells were fixed, DAPI stained and viewed by fluorescence microscopy.

Rpl11p-GFP showed strong nucleoplasmic accumulation 5 min after transfer to 37°C (data not shown) but the signal failed to concentrate in a nucleolar focus after 15, 30 or 60 min (Figure 9). Small nucleolar foci were observed in both double mutant strains, but they were observed in less than 5% of the cells (compared to more than 80% in the *sda1–2* single mutant) and only 60 min following temperature shift (data not shown). From these results we conclude that the intact TRAMP and exosome complexes are required for concentration of the pre-60S ribosomes in a subnucleolar focus.

Similar foci can be observed in other strains defective for ribosomal export

The export receptor Crm1p/Xpo1p is also required for the export of both the pre-40S and pre-60S ribosomal complexes (Ho *et al*, 2000; Gadal *et al*, 2001; Moy and Silver, 2002; Thomas and Kutay, 2003; Trotta *et al*, 2003). To assess whether the nucleolar focus of pre-ribosomes was specific to the *sda1–2* mutation, we tested strains carrying either the ts lethal *xpo1-1* mutation (Stade *et al*, 1997) or the *crm1^T539C* point mutation (Neville and Rosbash, 1999) at short time points following transfer to 37°C. Although the *crm1^T539C* strain was not ts-lethal (Neville and Rosbash, 1999), very similar effects on ribosome transport were seen with either mutation (shown for *crm1^T539C* in Figure 10). At 5 min after transfer to 37°C, the Rpl11p-GFP reporter showed accumulation within a crescent-shaped nuclear region immediately adjacent to the DAPI-stained nucleoplasm, indicating nucleolar or perinucleolar localization. By 15 min after transfer, the

Figure 9 Integrity of TRAMP and exosome is required to concentrate pre-ribosomes in the subnucleolar focus. *SDA1* and *sda1–2* strains were deleted for *RRP6* (**A**) or *TRF4* (**B**) genes (see Materials and methods) and transformed with pRpl11b-GFP. The resulting strains were pregrown at 23°C and shifted to 37°C for the times indicated. Cells were fixed, DAPI stained and viewed by fluorescence microscopy.

Figure 10 Pre-60S ribosomes form a focus in *crm1-1* mutant strains. Rpl11b-GFP was expressed in strains carrying either *HA-CRM1* or *HA-crm1^T539C*. The resulting strains were pregrown at 23°C and shifted to 37°C for the times indicated. Cells were fixed, DAPI stained and viewed by fluorescence microscopy.

staining was clearly enriched in a discrete focus, which persisted in the 30 min samples. Moreover, the accumulation of tagged r-protein reporters in a similar subnucleolar focus is also visible in some previously published images of strains with ribosomal export defects (Milkereit *et al*, 2001; Dong *et al*, 2005).

Discussion

Eucaryotic cells have developed many quality control systems to ensure the fidelity of gene expression. Here we describe a surveillance pathway that eliminates defective, nuclear-restricted 60S pre-ribosomal subunits. This process involves the addition of poly(A) tails to the targeted RNAs by the TRAMP4 complex prior to exosome-dependant degradation. We further identify a specific nucleolar substructure in which surveillance is likely to take place, and designate this region as the No-body.

We previously reported the identification of a family of ribosome synthesis factors that are largely comprised of HEAT-repeats and hypothesized their participation in the nucleo-cytoplasmic transport of ribosomal subunits, by homology to the importin-β/karyopherin-β family of HEAT-repeat containing transport factors (Dlakic and Tollervey, 2004; Oeffinger *et al*, 2004). Our demonstration that the HEAT-repeat protein Sda1p is required for the export of both subunits supports this model, since previous data provided no other evidence of a role for Sda1p in ribosome export. However, the available data do not allow us to clearly distinguish between a defect in the mechanism of export and a failure to acquire export competence. In strains carrying the fast-acting, ts-lethal *sda1–2* mutation (Zimmerman and Kellogg, 2001), strong nucleoplasmic accumulation of pre-40S and pre-60S ribosomes was visible in more than 80% of cells 5 min after shift to nonpermissive temperature. The onset of the ribosome export phenotype in *sda1–2* strains is much more rapid than previously reported in any mutant strain, and was observed before substantial alterations in the levels of either pre-rRNAs or rRNAs. The rapid onset and high penetrance of this phenotype offers the possibility of correlating the cell biology of pre-ribosome localization assessed by microscopy on individual cells, with analyses of RNA metabolism performed on the entire cell population.

Strains carrying *sda1–2* exhibited strong defects in pre-rRNA processing, particularly on the pathway of 60S ribosome synthesis. This suggests than, in addition to its role in export, Sda1p is required for pre-ribosomal processing and/or assembly. However, at least some of these defects probably result from the depletion of ribosome synthesis factors that are sequestered in nuclear-restricted pre-ribosomes. The very high flux of ribosome synthesis in yeast (2000 ribosomes/min in fast-growing strains) implies that the pool of free ribosome synthesis factors will be very rapidly depleted if recycling is impeded. Sda1p was shown to be associated with late pre-60S particles, but we did not detect its association with the 20S pre-rRNA component of pre-40S ribosomes. Many characterized ribosome synthesis factors are not retained in purified pre-ribosomes, and it is possible that Sda1p is lost from pre-40S particles during purification. However, it seems more likely that the defect in pre-40S export is indirect, possibly due to the sequestration in No-body localized pre-60S particles of shared export factors, for example, Rrp12p or

Xpo1p/Crm1p (Ho *et al*, 2000; Gadal *et al*, 2001; Moy and Silver, 2002; Thomas and Kutay, 2003; Trotta *et al*, 2003; Oeffinger *et al*, 2004). Such an indirect effect might explain why the pre-40S particles are apparently not subject to rapid nuclear degradation.

Pulse-labeling showed that despite an almost complete lack of 25S rRNA synthesis, the precursor RNAs were not accumulating to high levels, demonstrating the degradation of the 27SB pre-rRNA and 25S rRNA. In *sda1–2* strains lacking the exosome component Rrp6p or the TRAMP4 component Trf4p, the pre-rRNA processing defect was partially suppressed, showing the involvement of the TRAMP4 complex and nuclear exosome in the process. The role of the TRAMP complex was supported by the observation that the 25S rRNA and 27SB pre-rRNA undergo polyadenylation by Trf4p in the *sda1–2* strain at 37°C. Some hyperadenylation was seen in the *sda1–2* strain lacking Rrp6p, consistent with previous observations indicating that Rrp6p antagonizes polyadenylation by Trf4p (Kadaba *et al*, 2004; LaCava *et al*, 2005; Vanacova *et al*, 2005; Wyers *et al*, 2005; Houseley and Tollervey, 2006). We conclude that elimination of 60S pre-ribosomal RNAs by the exosome requires prior TRAMP4-dependant polyadenylation of the RNA substrates.

The nuclear-restricted pre-ribosomes showed striking enrichment in a nucleolar substructure, the No-body, in which the TRAMP and exosome complexes are also detected. In *sda1–2* strains lacking TRAMP or exosome components, the pre-60S ribosomes were stabilized and no longer accumulated in a focus, indicating a correlation between efficient pre-ribosome degradation and localization to this subnucleolar region. Poly(A)$^+$ RNA was also enriched in this focus, indicating that it represents the site of pre-rRNA polyadenylation and is therefore likely to be the site at which surveillance of the pre-ribosomes occurs. Notably, the nucleolar accumulation of polyadenylated RNA was previously observed in exosome (*mtr3-1*) and TRAMP (*mtr4*) mutants (Kadowaki *et al*, 1994, 1995). In particular, the *mtr4* mutant accumulated poly(A)$^+$ RNA in a single subnucleolar focus (Kadowaki *et al*, 1994). The TRAMP and exosome complexes are implicated in the surveillance of many other nuclear RNAs. Whether these surveillance activities are similarly localized remains to be determined.

In the cytoplasm, mRNA 5′ degradation and surveillance activities are preferentially localized in a discrete region termed the processing body (P-body); see Coller and Parker (2005) and references therein. It appears that the fate of the mRNA is determined within this structure, leading to either degradation or release back into the pool of translating mRNAs. In the *sda1–2* strain, pre-40S subunits, which are not subject to substantial degradation, were also enriched in the No-body. This suggests that pre-ribosomes that 'pass' surveillance can similarly be released from the No-body for productive processing.

It is unclear how the TRAMP complex differentiates between 'normal' pre-ribosomes and the nuclear-restricted particles. We speculate that one or more factors that normally associate with the pre-ribosomes can act to recruit the TRAMP complex, if not displaced by timely maturation. Such a 'fail-safe' mechanism would be conceptually similar to other surveillance pathways including nonsense-mediated decay (NMD), in which the human exon-junction complex (EJC) (Le Hir *et al*, 2000, 2001) or yeast Hrp1p (Kessler *et al*,

1997; Gonzalez *et al*, 2000) initiate degradation if retained on mRNAs. Analyses of pre-ribosome composition indicate that many synthesis factors are normally released at, or immediately prior to, transit through the NPC (Nissan *et al*, 2002; Saveanu *et al*, 2003). The pre-ribosomes accumulated in the *sda1–2* strains are likely to retain several inappropriate pre-ribosomal proteins, which could potentially recruit the degradation machinery.

In conclusion, we propose that in *sda1–2* strains exposed to nonpermissive temperature active surveillance of ribosome biogenesis is triggered, leading to the concentration of pre-ribosomes in the No-body, where aberrant particles are recognized and degraded. There have been many references to the existence of 'factories' for RNA synthesis, within which the synthesis machinery may concentrate to make maturation more efficient. We suggest that there is also a 'demolition site' for ribosomes, in which the exosome and the TRAMP complex are concentrated.

Materials and methods

Strains, plasmids, media and cloning techniques
For strains used and details of construction, see Supplementary Table S1. Standard procedures were used for the propagation and maintenance of yeast using YPD medium (1% yeast extract, 2% peptone and 2% glucose) or YNB medium (0.67% yeast nitrogen base, 0.5% $(NH_4)_2SO_4$ and 2% glucose) supplemented with the required amino acids.

Temperature shift of SDA1 and sda1–2 cells
As the response of the *sda1–2* strain to 37°C is very fast, we standardized the transfer to minimize the delay in culture warming. For microscopy, 25 ml of cells pregrown at 23°C were directly transferred to 250 ml flasks prewarmed in a water bath to 37°C. Aliquots were immediately fixed with paraformaldehyde. For larger cultures, 100 ml of cells were transferred to prewarmed 1 l flasks. Samples were placed in ice for 10 min before centrifugation.

RNA extraction and Northern hybridization
RNA extraction and Northern hybridization were performed as previously described (Beltrame and Tollervey, 1992). For high molecular weight RNA analysis, 5 μg of total of RNA were glyoxal denatured and resolved on a standard 1.2% agarose gel, as previously described (Sambrook and Russell, 2001). Low molecular weight RNA products were resolved on standard 8% polyacrylamide/8.3 M urea gels.

Selection of poly(A)$^+$ RNAs
Polyadenylated RNAs were purified from 200 μg of total RNAs using the 'PolyA Tract mRNA Isolation System IV' (Promega) as instructed by the supplier. The unbound and bound fractions were loaded on the gels in a ratio of 1:50.

Immunoprecipitations
Total cellular extracts were produced from strains expressing Sda1p-TAP and lacking a tagged protein. Cells frozen in liquid nitrogen were broken in a mortar. Immunoprecipitation and analysis of co-precipitated RNAs were performed as described (Dez *et al*, 2004). Total/immunoprecipitate ratios loaded were 1/20 for agarose gels and 1/10 for acrylamide gels.

Pulse-chase analysis
Metabolic labeling of pre-rRNA was performed as previously described (Tollervey *et al*, 1993) with the following modifications. The strains *SDA1*; *sda1–2*; *sda1–2, trf4Δ* and *sda1–2, rrp6Δ* were transformed with a plasmid containing the *ADE2* gene. Strains were pregrown in synthetic glucose medium lacking adenine at 23°C to an OD_{600} of 0.4 and were shifted to 37°C for 5 min. Cells were labeled with [8-^{3}H]adenine (TRK343, Amersham) for 2 min followed by a chase of excess cold adenine. Samples (1 ml) were collected at 1, 2, 5, 15, 30 and 60 min following the addition of cold adenine and cell pellets were frozen in liquid nitrogen. RNA was subsequently extracted and precipitated with ethanol.

Fluorescence microscopy
For fluorescence microscopy, cells were pregrown in YPD medium at 23°C to an OD_{600} of 0.3 and then shifted to 37°C. Aliquots were collected at the different time points and cells were fixed for 5 min in 4% paraformaldehyde at room temperature. After washing, the cells were mounted in medium containing DAPI (Vectashield, Vector Laboratories). For immunofluorescence, cells were fixed in 4% paraformaldehyde and spheroplasted with zymolase. Nop1p was detected using anti-Nop1p antibody (kindly provided by J Aris) (Henriquez *et al*, 1990) and a secondary goat anti-mouse antibody conjugated to Alexafluor 555 (Molecular Probes). FISH experiments were performed as described previously (Leger-Silvestre *et al*, 2004) using Cy3-labeled ITS2 and Cy5-labeled oligo(dT) probes.

Fractionation of yeast extracts on glycerol gradients
A total cellular extract was prepared as described in the 'immunoprecipitations' paragraph from the *SDA1* and *sda1.2* strains expressing Rpl11b-GFP or Rps2-GFP. In total, 0.5 ml of extract corresponding to 5 mg of proteins was loaded on a 10–30% glycerol gradient and centrifuged for 12.5 h at 23 000 r.p.m. in an SW40 rotor. A total of 18 fractions were collected from the top. Proteins and RNAs were extracted from each fraction and, respectively, subjected to Western blot and Northern blot analysis.

Production of total proteins extracts and Western blot analysis
Total proteins extracts and Western blot analysis were performed as previously described (Dez *et al*, 2004). Nop1p was detected using monoclonal anti-Nop1p antibody and Rpl11b-TAP by the use of rabbit PAP. Rps2-GFP and Rpl11b-GFP were detected using monoclonal anti-GFP antibody (Clontech).

Supplementary data
Supplementary data are available at *The EMBO Journal* Online.

References

Allmang C, Kufel J, Chanfreau G, Mitchell P, Petfalski E, Tollervey D (1999) Functions of the exosome in rRNA, snoRNA and snRNA synthesis. *EMBO J* **18:** 5399–5410

Allmang C, Mitchell P, Petfalski E, Tollervey D (2000) Degradation of ribosomal RNA precursors by the exosome. *Nucleic Acids Res* **28:** 1684–1691

Andrade MA, Petosa C, O'Donoghue SI, Muller CW, Bork P (2001) Comparison of ARM and HEAT protein repeats. *J Mol Biol* **309:** 1–18

Babbio F, Farinacci M, Saracino F, Carbone ML, Privitera E (2004) Expression and localization studies of hSDA, the human ortholog of the yeast SDA1 gene. *Cell Cycle* **3:** 486–490

Baßler J, Grandi P, Gadal O, Leßmann T, Petfalski E, Tollervey D, Lechner J, Hurt E (2001) Identification of a 60S pre-ribosomal particle that is closely linked to nuclear export. *Mol Cell* **8:** 517–529

Beltrame M, Tollervey D (1992) Identification and functional analysis of two U3 binding sites on yeast pre-ribosomal RNA. *EMBO J* **11:** 1531–1542

Bertrand E, Chartrand P, Schaefer M, Shenoy SM, Singer RH, Long RM (1998) Localization of ASH1 mRNA particles in living yeast. *Mol Cell* **2:** 437–445

Bousquet-Antonelli C, Presutti C, Tollervey D (2000) Identification of a regulated pathway for nuclear pre-mRNA turnover. *Cell* **102:** 765–775

Buscemi G, Saracino F, Masnada D, Carbone ML (2000) The *Saccharomyces cerevisiae* SDA1 gene is required for actin cytoskeleton organization and cell cycle progression. *J Cell Sci* **113:** 1199–1211

Coller J, Parker R (2005) General translational repression by activators of mRNA decapping. *Cell* **122:** 875–886

de la Cruz J, Kressler D, Linder P (2003) Ribosomal subunit assembly. In Olson MOJ (ed) *The Nucleolus*, pp 262–290. Dordrecht/New York: KluwerAcademic/Plenum Publishers

de la Cruz J, Kressler D, Tollervey D, Linder P (1998) Dob1p (Mtr4p) is a putative ATP-dependent RNA helicase required for the 3′ end formation of 5.8S rRNA in *Saccharomyces cerevisiae*. *EMBO J* **17:** 1128–1140

Dez C, Froment C, Noaillac-Depeyre J, Monsarrat B, Caizergues-Ferrer M, Henry Y (2004) Npa1p, a component of very early pre-60S ribosomal particles, associates with a subset of small nucleolar RNPs required for peptidyl transferase center modification. *Mol Cell Biol* **24:** 6324–6337

Dez C, Tollervey D (2004) Ribosome synthesis meets the cell cycle. *Curr Opin Microbiol* **7:** 631–637

Dlakic M, Tollervey D (2004) The Noc proteins involved in ribosome synthesis and export contain divergent HEAT repeats. *RNA* **10:** 351–354

Dong J, Lai R, Jennings JL, Link AJ, Hinnebusch AG (2005) The novel ATP-binding cassette protein ARB1 is a shuttling factor that stimulates 40S and 60S ribosome biogenesis. *Mol Cell Biol* **25:** 9859–9873

Fang F, Hoskins J, Butler JS (2004) 5-Fluorouracil enhances exosome-dependent accumulation of polyadenylated rRNAs. *Mol Cell Biol* **24:** 10766–10776

Fromont-Racine M, Senger B, Saveanu C, Fasiolo F (2003) Ribosome assembly in eukaryotes. *Gene* **313:** 17–42

Gadal O, Strauss D, Kessl J, Trumpower B, Tollervey D, Hurt E (2001) Nuclear export of 60s ribosomal subunits depends on Xpo1p and requires a nuclear export sequence-containing factor, Nmd3p, that associates with the large subunit protein Rpl10p. *Mol Cell Biol* **21:** 3405–3415

Gavin AC, Bosche M, Krause R, Grandi P, Marzioch M, Bauer A, Schultz J, Rick JM, Michon AM, Cruciat CM, Remor M, Hofert C, Schelder M, Brajenovic M, Ruffner H, Merino A, Klein K, Hudak M, Dickson D, Rudi T, Gnau V, Bauch A, Bastuck S, Huhse B, Leutwein C, Heurtier MA, Copley RR, Edelmann A, Querfurth E, Rybin V, Drewes G, Raida M, Bouwmeester T, Bork P, Seraphin B, Kuster B, Neubauer G, Superti-Furga G (2002) Functional organization of the yeast proteome by systematic analysis of protein complexes. *Nature* **415:** 141–147

Gonzalez CI, Ruiz-Echevarria MJ, Vasudevan S, Henry MF, Peltz SW (2000) The yeast hnRNP-like protein Hrp1/Nab4 marks a transcript for nonsense-mediated mRNA decay. *Mol Cell* **5:** 489–499

Gorlich D, Seewald MJ, Ribbeck K (2003) Characterization of Ran-driven cargo transport and the RanGTPase system by kinetic measurements and computer simulation. *EMBO J* **22:** 1088–1100

Grandi P, Rybin V, Bassler J, Petfalski E, Strauss D, Marzioch M, Schafer T, Kuster B, Tschochner H, Tollervey D, Gavin AC, Hurt E (2002) 90S pre-ribosomes include the 35S pre-rRNA, the U3 snoRNP, and 40S subunit processing factors but predominantly lack 60S synthesis factors. *Mol Cell* **10:** 105–115

Haracska L, Johnson RE, Prakash L, Prakash S (2005) Trf4 and Trf5 proteins of *Saccharomyces cerevisiae* exhibit poly(A) RNA polymerase activity but no DNA polymerase activity. *Mol Cell Biol* **25:** 10183–10189

Henriquez R, Blobel G, Aris JP (1990) Isolation and sequencing of NOP1. A yeast gene encoding a nucleolar protein homologous to a human autoimmune antigen. *J Biol Chem* **265:** 2209–2215

Hilleren P, McCarthy T, Rosbash M, Parker R, Jensen TH (2001) Quality control of mRNA 3′-end processing is linked to the nuclear exosome. *Nature* **413:** 538–542

Ho JH, Kallstrom G, Johnson AW (2000) Nmd3p is a Crm1p-dependent adapter protein for nuclear export of the large ribosomal subunit. *J Cell Biol* **151:** 1057–1066

Houseley J, Tollervey D (2006) Yeast Trf5p is a nuclear poly(A) polymerase. *EMBO Rep* **7:** 205–211

Inoue K, Mizuno T, Wada K, Hagiwara M (2000) Novel RING finger proteins, Air1p and Air2p, interact with Hmt1p and inhibit the arginine methylation of Npl3p. *J Biol Chem* **275:** 32793–32799

Kadaba S, Krueger A, Trice T, Krecic AM, Hinnebusch AG, Anderson J (2004) Nuclear surveillance and degradation of hypomodified initiator tRNAMet in *S. cerevisiae*. *Genes Dev* **18:** 1227–1240

Kadowaki T, Chen S, Hitomi M, Jacobs E, Kumagai C, Liang S, Schneiter R, Singleton D, Wisniewska J, Tartakoff AM (1994) Isolation and characterization of *Saccharomyces cerevisiae* mRNA transport-defective (mtr) mutants. *J Cell Biol* **126:** 649–659 (published erratum appears in *J Cell Biol* 1994 Sep; **1126**(1996): 1627)

Kadowaki T, Schneiter R, Hitomi M, Tartakoff AM (1995) Mutations in nucleolar proteins lead to nucleolar accumulation of polyA + RNA in *Saccharomyces cerevisiae*. *Mol Biol Cell* **6:** 1103–1110

Kessler MM, Henry MF, Shen E, Zhao J, Gross S, Silver PA, Moore CL (1997) Hrp1, a sequence-specific RNA-binding protein that shuttles between the nucleus and the cytoplasm, is required for mRNA 3′-end formation in yeast. *Genes Dev* **11:** 2545–2556

Kuai L, Fang F, Butler JS, Sherman F (2004) Polyadenylation of rRNA in *Saccharomyces cerevisiae*. *Proc Natl Acad Sci USA* **101:** 8581–8586

LaCava J, Houseley J, Saveanu C, Petfalski E, Thompson E, Jacquier A, Tollervey D (2005) RNA degradation by the exosome is promoted by a nuclear polyadenylation complex. *Cell* **121:** 713–724

Le Hir H, Gatfield D, Izaurralde E, Moore MJ (2001) The exon–exon junction complex provides a binding platform for factors involved in mRNA export and nonsense-mediated mRNA decay. *EMBO J* **20:** 4987–4997

Le Hir H, Moore MJ, Maquat LE (2000) Pre-mRNA splicing alters mRNP composition: evidence for stable association of proteins at exon–exon junctions. *Genes Dev* **14:** 1098–1108

Leger-Silvestre I, Milkereit P, Ferreira-Cerca S, Saveanu C, Rousselle JC, Choesmel V, Guinefoleau C, Gas N, Gleizes PE (2004) The ribosomal protein Rps15p is required for nuclear exit of the 40S subunit precursors in yeast. *EMBO J* **23:** 2336–2347

Liang S, Hitomi M, Hu YH, Liu Y, Tartakoff AM (1996) A DEAD-box-family protein is required for nucleocytoplasmic transport of yeast mRNA. *Mol Cell Biol* **16:** 5139–5146

Libri D, Dower K, Boulay J, Thomsen R, Rosbash M, Jensen TH (2002) Interactions between mRNA export commitment, 3′-end quality control, and nuclear degradation. *Mol Cell Biol* **22:** 8254–8266

Milkereit P, Gadal O, Podtelejnikov A, Trumtel S, Gas N, Petfalski E, Tollervey D, Mann M, Hurt E, Tschochner H (2001) Maturation and intranuclear transport of pre-ribosomes requires Noc proteins. *Cell* **105:** 499–509

Milkereit P, Strauss D, Bassler J, Gadal O, Kuhn H, Schutz S, Gas N, Lechner J, Hurt E, Tschochner H (2003) A Noc complex specifically involved in the formation and nuclear export of ribosomal 40 S subunits. *J Biol Chem* **278:** 4072–4081

Milligan L, Torchet C, Allmang C, Shipman T, Tollervey D (2005) A nuclear surveillance pathway for mRNAs with defective polyadenylation. *Mol Cell Biol* **25:** 9996–10004

Mitchell P, Petfalski E, Shevchenko A, Mann M, Tollervey D (1997) The exosome; a conserved eukaryotic RNA processing complex containing multiple 3′→5′ exoribonuclease activities. *Cell* **91:** 457–466

Moy TI, Silver PA (2002) Requirements for the nuclear export of the small ribosomal subunit. *J Cell Sci* **115:** 2985–2995

Neville M, Rosbash M (1999) The NES-Crm1p export pathway is not a major mRNA export route in *Saccharomyces cerevisiae*. *EMBO J* **18:** 3746–3756

Nissan TA, Bassler J, Petfalski E, Tollervey D, Hurt E (2002) 60S pre-ribosome formation viewed from assembly in the nucleolus until export to the cytoplasm. *EMBO J* **21:** 5539–5547

Oeffinger M, Dlakic M, Tollervey D (2004) A pre-ribosome-associated HEAT-repeat protein is required for export of both ribosomal subunits. *Genes Dev* **18:** 196–209

Ribbeck K, Gorlich D (2002) The permeability barrier of nuclear pore complexes appears to operate via hydrophobic exclusion. *EMBO J* **21:** 2664–2671

Rigaut G, Shevchenko A, Rutz B, Wilm M, Mann M, Seraphin B (1999) A generic protein purification method for protein complex characterization and proteome exploration. *Nat Biotechnol* **17:** 1030–1032

Saitoh S, Chabes A, McDonald WH, Thelander L, Yates JR, Russell P (2002) Cid13 is a cytoplasmic poly(A) polymerase that regulates ribonucleotide reductase mRNA. *Cell* **109:** 563–573

Sambrook J, Russell D (2001) *Molecular cloning*. Cold Spring Harbor, New York: Cold Spring Harbor Laboratory Press

Saveanu C, Namane A, Gleizes PE, Lebreton A, Rousselle JC, Noaillac-Depeyre J, Gas N, Jacquier A, Fromont-Racine M (2003) Sequential protein association with nascent 60S ribosomal particles. *Mol Cell Biol* **23:** 4449–4460

Stade K, Ford CS, Guthrie C, Weis K (1997) Exportin 1 (Crm1p) is an essential nuclear export factor. *Cell* **90:** 1041–1050

Stage-Zimmermann T, Schmidt U, Silver PA (2000) Factors affecting nuclear export of the 60S ribosomal subunit *in vivo*. *Mol Biol Cell* **11:** 3777–3789

Thomas F, Kutay U (2003) Biogenesis and nuclear export of ribosomal subunits in higher eukaryotes depend on the CRM1 export pathway. *J Cell Sci* **116:** 2409–2419

Tollervey D, Lehtonen H, Jansen R, Kern H, Hurt EC (1993) Temperature-sensitive mutations demonstrate roles for yeast fibrillarin in pre-rRNA processing, pre-rRNA methylation, and ribosome assembly. *Cell* **72:** 443–457

Torchet C, Bousquet-Antonelli C, Milligan L, Thompson E, Kufel J, Tollervey D (2002) Processing of 3′ extended read-through transcripts by the exosome can generate functional mRNAs. *Mol Cell* **9:** 1285–1296

Trotta CR, Lund E, Kahan L, Johnson AW, Dahlberg JE (2003) Coordinated nuclear export of 60S ribosomal subunits and NMD3 in vertebrates. *EMBO J* **22:** 2841–2851

van Hoof A, Lennertz P, Parker R (2000) Yeast exosome mutants accumulate 3′-extended polyadenylated forms of U4 small nuclear RNA and small nucleolar RNAs. *Mol Cell Biol* **20:** 441–452

Vanacova S, Wolf J, Martin G, Blank D, Dettwiler S, Friedlein A, Langen H, Keith G, Keller W (2005) A new yeast poly(A) polymerase complex involved in RNA quality control. *PLoS Biol* **3:** e189

Venema J, Tollervey D (1999) Ribosome synthesis in *Saccharomyces cerevisiae*. *Ann Rev Gen* **33:** 261–311

Wyers F, Rougemaille M, Badis G, Rousselle JC, Dufour ME, Boulay J, Regnault B, Devaux F, Namane A, Seraphin B, Libri D, Jacquier A (2005) Cryptic Pol II transcripts are degraded by a nuclear quality control pathway involving a new poly(A) polymerase. *Cell* **121:** 725–737

Zanchin NI, Goldfarb DS (1999) The exosome subunit Rrp43p is required for the efficient maturation of 5.8S, 18S and 25S rRNA. *Nucleic Acids Res* **27:** 1283–1288

Zenklusen D, Vinciguerra P, Wyss JC, Stutz F (2002) Stable mRNP formation and export require cotranscriptional recruitment of the mRNA export factors Yra1p and Sub2p by Hpr1p. *Mol Cell Biol* **22:** 8241–8253

Zimmerman ZA, Kellogg DR (2001) The Sda1 protein is required for passage through start. *Mol Biol Cell* **12:** 201–219